Biol. Chem., Vol. 388, pp. 561–568, June 2007 • Copyright © by Walter de Gruyter • Berlin • New York. DOI 10.1515/BC.2007.074

Anti-innexin 2 aptamers specifically inhibit the heterologous interaction of the innexin 2 and innexin 3 carboxyl-termini *in vitro*

Martin Knieps[1], Sonja Herrmann[1], Corinna Lehmann[2], Birgit Löer[2], Michael Hoch[2] and Michael Famulok[1,*]

[1] LIMES Institute, Program Unit Chemical Biology and Medicinal Chemistry, c/o Kekulé Institute for Organic Chemistry and Biochemistry, University of Bonn, Gerhard-Domagk-Straße 1, D-53121 Bonn, Germany
[2] LIMES Institute, Program Unit Development and Genetics, Laboratory for Molecular Developmental Biology, University of Bonn, Meckenheimer Allee 169, D-53115 Bonn, Germany

* Corresponding author
e-mail: m.famulok@uni-bonn.de

Abstract

We recently demonstrated that heteromerization of innexins 2 and 3 from *Drosophila melanogaster* (*Dm*) is crucial for epithelial organization and polarity of the embryonic epidermis. Both innexins are thought to interact via their C-terminal cytoplasmic domains during the assembly of heteromeric gap junction channels. However, the mechanisms that control heteromeric versus homomeric channel formation are still largely unknown. Here we report the isolation of both non-modified and 2′-fluoro-2′-deoxy-modified RNA anti-innexin 2 aptamers by *in vitro* selection. The aptamers bind to a proximal epitope on the carboxyl-tail of *Dm* innexin 2 protein and specifically inhibit the heterologous interaction of innexin 2 and innexin 3 carboxyl-termini *in vitro*. These domain-specific inhibitors represent the first step towards functional studies focusing on the activity of these domains *in vivo*.

Keywords: aptamer; *Drosophila*; gap junctions; innexin 2; innexin 3; *in vitro* selection.

Introduction

Gap junction communication channels enable the integration of metabolic and signaling activities by allowing the direct intercellular exchange of cytoplasmic small molecules, ions, and metabolites. They are clustered in spatial micro-domains in the plasma membranes of neighboring cells at regions of cell adhesion. Gap junction channel proteins of vertebrates are encoded by the *connexin* multi-gene family, which consists of 20 members in mice and 21 in humans (Söhl and Willecke, 2004). Connexins oligomerize to form hexameric hemichannel subunits, two of which, contributed by each of the opposing cells, dock head-to-head extracellularly to form a double membrane-spanning intercellular channel (Martin and Evans, 2004; Segretain and Falk, 2004). Because tissues usually express different connexin isoforms, cells can potentially form homo- or heteromeric hemichannels that can assemble into even more complex homotypic or heterotypic channels. In this way, combinatorial assembly of relatively few protein isoforms might result in a highly diverse variety of differently composed gap junctions, which might enable cells to regulate gap junction communication in a highly complex fashion. Thus, variation in connexin stoichiometry might determine the selectivity of channels, which may allow cells to dynamically regulate intercellular properties. Whether such different types of hemichannels occur in the same cell and what function they may serve *in vivo* are still essentially unclear (Kumar and Gilula, 1996). Invertebrate gap junction proteins are encoded by the *innexin* multi-gene family (Phelan et al., 1998; Bauer et al., 2005). Innexins span the membrane four times (TM1–TM4) and form two large extracellular loops. The amino- (NT) and carboxyl-termini (CT) and the loop between TM2 and TM3 (CL) are located in the cytoplasm (Figure 1A). Analogously, six innexins are supposed to assemble into a hemichannel (innexon) in a homo- or probably heteromeric fashion (Figure 1B). Thus, invertebrate innexins resemble connexin channel formation in vertebrates (Phelan and Starich, 2001; Bauer et al., 2005; Lehmann et al., 2006).

In *Drosophila melanogaster*, eight innexins have been identified that share no sequence similarities to mammalian connexins, but show some sequence similarities to the recently discovered pannexin protein family (Stebbings et al., 2002; Bruzzone et al., 2003; Söhl and Willecke, 2004). With respect to structural similarities, innexin NT, CL or CT may nonetheless fulfill similar functions to corresponding intercellular domains of connexins. Investigation of connexin CT domains, for example, led to the discovery of β-catenin (Ai et al., 2000), zonula occludens (ZO-1) (Giepmans and Moolenaar, 1998; Toyofuku et al., 2001; Sorgen et al., 2004), v- and c-src (Duffy et al., 2001), tubulin (Giepmans et al., 2001) and caveolin-1 (Schubert et al., 2002) as presumptive direct interaction partners. In *D. melanogaster*, armadillo (β-catenin), DE-cadherin and probably the septate junction protein coracle have been identified to interact with innexin 2 (Bauer et al., 2004). Furthermore, for connexins, intramolecular interactions such as dimerization of CT domains or binding of the carboxyl tail to a receptor domain in the cytoplasmic loop in homologous and heterologous hemichannels were discussed in the context of a ‘ball and chain’ model for regulation of the gating of gap junctions (Anumonwo et al., 2001; Duffy et al., 2002; Sorgen et al., 2004). However, only limited biochemical evidence is available on innexin oligomeriza-

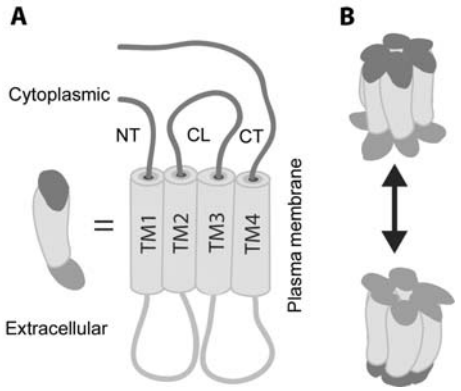

Figure 1 Topology of innexin 2 (Ix2) gap junction channels.
(A) Topology of innexins (TM, transmembrane domain; NT, N-terminal domain; CL, cytoplasmic loop; CT, cytoplasmic tail). (B) Docking of two half-channels (innexons) each composed of six subunits (innexins) to form a gap junction channel.

tion, and molecular or biochemical evidence for heteromeric hemichannels and for heterotypic gap junctions in *Drosophila* is still scarce.

Recently we have shown that innexins 2 and 3 form mixed channels that control the localization of adherens junctional core proteins required for epithelial organization in the *Drosophila* epidermis. By applying co-immunoprecipitation analyses, transgenesis, and surface plasmon resonance studies, we observed that innexins 2 and 3 interact *in vitro* and *in vivo* via their CT cytoplasmic domains, thereby providing strong evidence for a direct and functional interaction between two invertebrate innexins (Lehmann et al., 2006).

To provide further evidence of a domain-specific functional role of innexins 2 and 3 in *Drosophila*, we searched for domain-specific inhibitors of these proteins that could be applied to study the function of the domains within their natural expression status. Aptamers have been successfully applied to modify protein functions inside cells (Blind et al., 1999; Shi et al., 1999; Mayer et al., 2001; Famulok and Verma, 2002; Theis et al., 2004; Famulok and Mayer, 2005; Choi et al., 2006). However, to the best of our knowledge, intercellular domains of multi-membrane-spanning proteins or protein complexes have yet not been investigated using an aptamer approach. Here, we report the selection of both non-modified and 2′-fluoro-2′-deoxy-modified RNA aptamers binding to a proximal epitope on the carboxyl tail of *Dm* innexin 2 protein. These aptamers specifically inhibit the heterologous interaction of innexin 2 and innexin 3 CTs *in vitro*.

Results

Selection of aptamers binding the innexin 2 carboxyl tail

Detailed sequence comparison of eight *D. melanogaster* innexins revealed the CTs as regions with the highest variability within the highly homologous members of this protein family (Stebbings et al., 2002). Thus, to select RNA aptamers specific for an intercellular domain of *Dm* innexin 2, we used a biotinylated version of a peptide fragment with low sequence conservation derived from the carboxyl tail (Bio-Ix2CTept1) for aptamer selections (Figure 2). A pool of approximately 1.5×10^{14} different DNA molecules was subjected to T7 polymerase transcription using either natural nucleoside triphosphates (NTPs) or 2′-fluoro-2′-deoxy pyrimidine triphosphates, together with purine triphosphates, to yield 2′-fluoro-modified RNAs with improved stability towards nucleases (Pieken et al., 1991; Lin et al., 1994; Proske et al., 2002b). Two selections were performed in parallel to isolate both unmodified RNA aptamers and 2′-fluoro-modified aptamers, which bound to Bio-Ix2CTept1 immobilized on streptavidin agarose.

After 12 selection cycles with unmodified RNA (OU), and 10 cycles in the selection with modified RNA (FS), individual members of the libraries were cloned and sequenced. Figure 3A lists the most abundant sequences. Several conserved sequence motifs were surprisingly predominant in both selections. A GGNTAAGGT motif is present in the most frequent sequences of both enriched pools, whereas most of the other sequences contain the G- and U-rich motifs UUGGGU and GUGGGGGGUCG with small variations. To compare the affinities of the enriched pools with those of individual sequences, we determined their dissociation constants (K_d values) by filter binding assays using biotinylated Ix2CTept1 immobilized on streptavidin (Figure 3B). Aptamer sequences bound the peptide-streptavidin complex with K_d values in the mid-nanomolar range and showed no significant binding to streptavidin alone (Table 1). However, when a His_6-tagged version of the complete innexin 2 CT (His-Ix2CT) was used, the same aptamers exhibited significantly reduced affinity, while clone FS2 still showed tight binding (data not shown). Additional binding studies revealed that this effect was caused by the absence of streptavidin, which appeared to be partially utilized by these aptamers, in addition to the innexin 2 epitope, to achieve tight binding (data not shown).

To generate non-modified RNA aptamers that bind to Ix2CT independent of the presence of streptavidin, a new library was created by 30 cycles of mutagenic PCR of

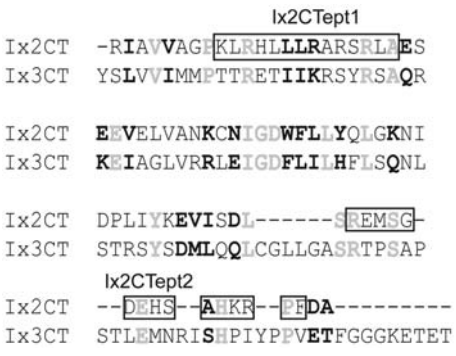

Figure 2 Sequence comparison of Ix2- and Ix3CT using ClustalW.
Identities (gray) and similarities (bold) are highlighted. The 14-aa-long peptide fragment Ix2CTept1 (boxed sequence) was chosen for aptamer selection. Ix2CTept2 served as a negative control in filter binding assays.

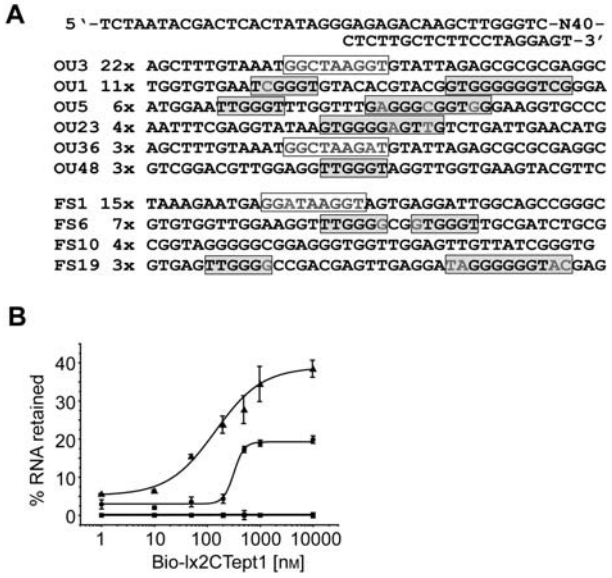

Figure 3 Sequences and affinity curves of aptamers selected for binding to Bio-Ix2CTept1/streptavidin.
(A) During selection, two different aptamer species sharing consensus motifs were evolved. Sequences of aptamers binding to the streptavidin/Bio-Ix2CTept1 complex are given with name, abundance and sequence of the random region N40. Pool 'I-40' sequence is written at the top. Common sequence motifs are boxed (white/gray shade); point mutations from the consensus are in gray. (B) Exemplary filter-binding assay of aptamers shown in panel (A) with Bio-Ix2CTept1 captured on streptavidin: (■) unmodified, unselected pool of selection round 0; (●) OU3 RNA; (▲) unmodified RNA from final pool of selection round 12.

the two aptamer sequences OU1 and OU3 at a mutation rate of 2% (Cadwell and Joyce, 1992, 1994) for use in a re-selection. During re-selection, RNAs with the ability to bind GST-Ix2CT were specifically eluted with excess His-Ix2CT to increase the stringency for evolution towards Ix2CT binders. Sequencing of the library after three cycles resulted in two new predominant sequences (Figure 4A). The re-selected sequences still contained the consensus motifs UUGGGU and GUGGGGGGUCG of their parent aptamers, with slight changes, but showed otherwise significant differences to OU1 and OU3, respectively. In contrast to the previously selected aptamers, these RNAs bound His-Ix2CT with nanomolar affinity (Figure 4B, right panel), but had lost their ability to bind to the Bio-Ix2CTept1-streptavidin complex (Figure 4B, left panel). Thus, the re-selection led to significant improvement of the selected aptamer with respect to target specificity.

Shortened aptamers are sufficient to bind His-Ix2CT

We next determined the minimal aptamer sequences required for His-Ix2CT binding. Gradually shortened versions of RE3A, RE3G and FS2 were produced by *in vitro* transcription and their affinities were tested in filter-binding assays (Table 2). The shortening of the sequences was combined with small modifications at the 5′- and 3′-ends to maintain the 5′-G triplet required for efficient yields during transcription with T7 RNA polymerase. Both RE3A and RE3G fold into compact paired structures, with only a few short G and U-rich loops (Figure 5), as suggested by the free-energy-minimized secondary structures calculated by the Mfold algorithm (Zuker, 2003). Both RE3G and FS2 could be shortened to 45 and 47 nt, respectively, without significant loss of binding affinity (Figure 5, Table 2). In addition, we successfully replaced the single A in sequence RE3G by a G to generate what is, to the best of our knowledge, the first RNA aptamer (RE3G45S) consisting of only three different nucleotides. This is more than just a simple anecdotal result, because functional RNAs composed of a reduced set of only three or even two nucleotides have implications for early evolution in a hypothetical RNA world (Rogers and Joyce, 1999, 2001; Reader and Joyce, 2002). Interestingly, the selected sequences display high G-content, especially the consensus sequences. This raises the possibility that RE3G might form a G-quadruplex scaffold. RE3A could be reduced to 60 nt, whereas the 45-mer showed lower binding affinity to His-Ix2CT (Figure 5). Dissociation constants measured for shortened and full-length aptamers are summarized in Table 2.

Aptamers can recognize full-length innexin 2

Pull-down experiments with biotinylated RNA were performed to further validate the specificity and binding properties of aptamers towards innexin 2. Labeled innexin 2 and innexin 3 were produced by coupled *in vitro* transcription/translation reactions in the presence of

Table 1 Dissociation constants of various aptamer and pool RNAs as determined in filter binding assays.

Aptamer	K_d (nM)[a]			
	Streptavidin+Bio-Ix2CTept1	Streptavidin+Bio-Ix2CTept2	Streptavidin	His-Ix2CT
OU1	44±4	>5000	>5000	>2000
OU3	276±95	>5000	>5000	>2000
OU5	112±30	>5000	>5000	>2000
Pool 12 (OU)	115±19	>5000	>5000	>2000
Pool 0	>5000	>5000	>5000	>2000
FS1	203±71	>5000	>5000	>2000
FS2	226±30	>5000	>5000	84±12

[a]RNA sequences (OU1; OU3; FS1; FS2) bind to Bio-Ix2CTept1 immobilized on streptavidin in a concentration-dependent fashion, whereas the unselected library (Pool 0) does not. RNAs selected for binding to this epitope neither bound to streptavidin alone, nor the streptavidin-immobilized epitope Bio-Ix2CTept2. The complete innexin 2 C-terminal domain fused to a His_6-tag (His-Ix2CT) is only bound by the aptamer FS2.

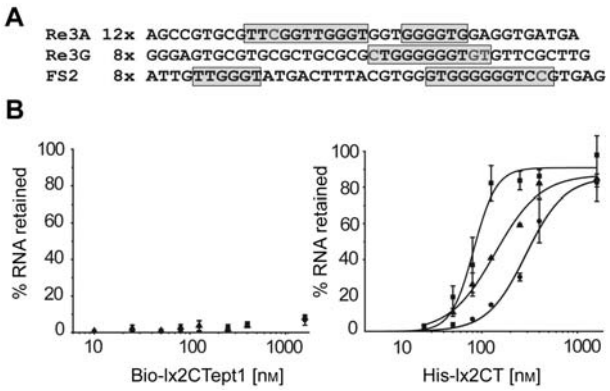

Figure 4 Sequences and affinity curves of aptamers re-selected for binding to His-Ix2CT.
(A) Random regions of re-selected aptamers binding to His-Ix2CT. (B) Filter-binding assays of aptamers shown in (A) with Bio-Ix2CTept1/streptavidin (left panel) and His-Ix2CT (right panel). (■) FS2, 2′-fluoro-modified RNA; (●) RE3A RNA; (▲) RE3G RNA.

[35S]-Pro-mix. Fractions bound to biotinylated RNA immobilized on streptavidin agarose were directly loaded onto SDS-PAGE after elution. Bands in the autoradiogram indicate that the re-selected aptamers RE3A and RE3G could recognize full-length innexin 2 and discriminate it from innexin 3 (Figure 6). A negative control sequence and an aptamer for Bio-Ix2CTept1-streptavidin complex (OU-1) were unable to bind innexin 2 in this assay.

Aptamers inhibit the interaction of innexin 2CT and innexin 3CT *in vitro*

Previously we investigated the interactions of isolated innexin 2 and innexin 3 intercellular domains using surface plasmon resonance (Lehmann et al., 2006). Here we established GST pull-down assays to provide further evidence of the specificity of these interactions.

In vitro translated [35S]-labeled innexin 2 fused to a Myc tag (Myc-Ix2) was incubated with GST-tagged innexin domains bound to glutathione-Sepharose beads. GST immobilized in the same way was used as a negative control. The eluted protein complexes were resolved by SDS-PAGE and visualized by autoradiography (Figure 7). When *in vitro*-translated [35S]-labeled innexin 2 was incubated with GST fusion proteins of the intracellular domains of innexins 2 and 3, binding could only be

Table 2 Dissociation constants of re-selected aptamers RE3A, RE3G, and shortened versions thereof, as determined in filter binding assays.

RNA[a]	Length (nt)	K_d (nM) His-Ix2CT
RE3A	79	308±18
RE3A60	60	212±27
RE3A45	45	>500
RE3G	79	222±36
RE3G45	45	343±54
RE3G45S	45	172±8
FS2-47	47	120±12

[a]RNA sequences binding to His(Xa)-Ix2CT.

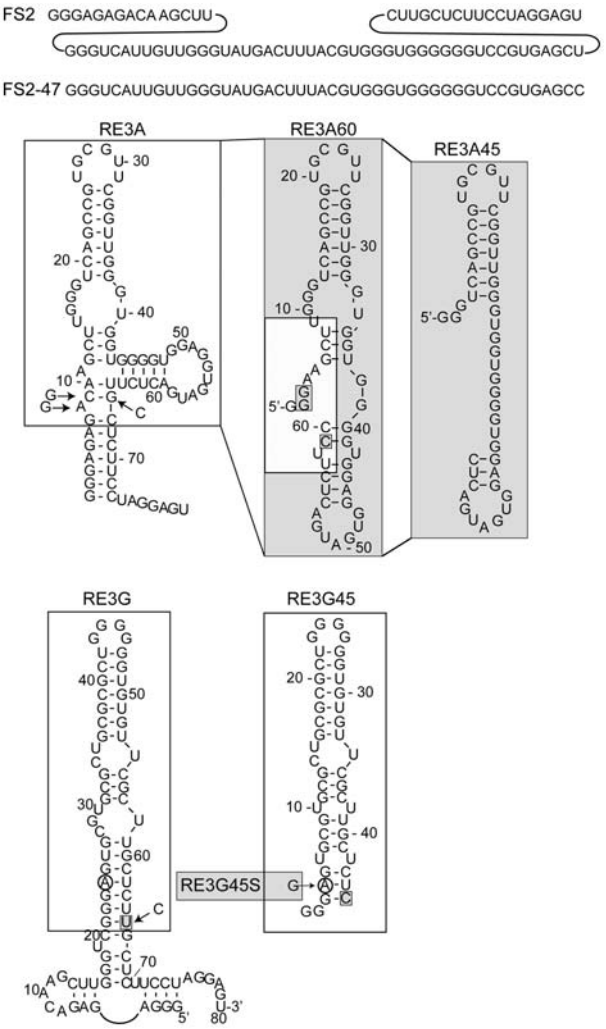

Figure 5 Proposed secondary structures of aptamers and the respective minimal motifs.
Secondary structures were calculated using Mfold. G→A replacement of one nucleotide in RE3G45 resulted in an aptamer (RE3G45S) lacking adenosine. Additional modifications in comparison to full-length aptamers (79 nt) were introduced to increase the folding stability (arrows), and are shaded in gray.

detected to the GST-innexin 2 cytoplasmic loop (GST-Ix2CL) and the GST-innexin 3 cytoplasmic tail (GST-Ix3CT). A weak interaction was also observed for the GST-innexin 3 cytoplasmic loop (GST-Ix3CL), but not to GST or any of the other fusion constructs (Figure 7A). These results correlate well with our previous measure-

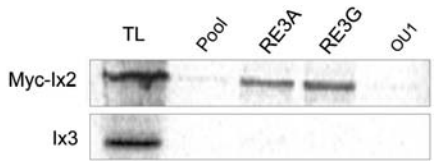

Figure 6 Re-selected aptamers specifically pull down innexin 2.
Aptamers discriminate innexin 2 from innexin 3. *In vitro* translated Myc-tagged Ix2 and Ix3 were incubated with biotinylated aptamers bound to streptavidin agarose. Analysis was by SDS-PAGE and autoradiography. TL, input of translation per pull-down assay.

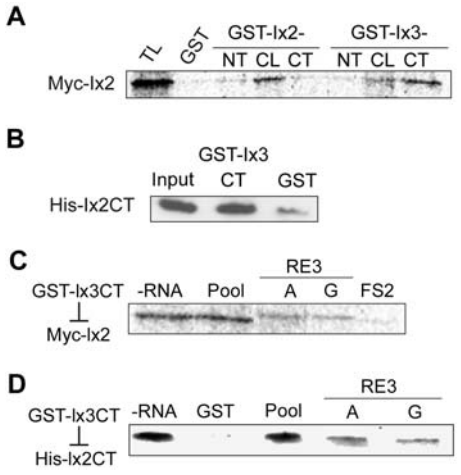

Figure 7 Pull-down experiments confirm the interaction of the innexin 2 C-terminus with the innexin 3 cytoplasmic tail.
(A) GST pull-down assay of *in vitro* translated Myc-Ix2 with intercellular domains of Ix2 and Ix3. Ix2CL, Ix3CL and Ix3CT were identified as possible interaction partners of Ix2CT. (B) His-Ix2CT is specifically precipitated by GST-Ix3CT, confirming the interaction of the cytoplasmic tails. For the detection of bound His-Ix2CT in Western blots, an α-penta-His-specific monoclonal antibody was used. (C) Inhibition of MycIx2/GST-Ix3CT interaction by aptamers. GST pull-down of Myc-Ix2 by GST-Ix3CT is inhibited in presence of the re-selected aptamers RE3A, RE3G, and by FS2, but not by the unselected pool 0 RNA. '-RNA', without RNA. (D) Inhibition of His-Ix2CT/GST-Ix3CT interaction by aptamers RE3A and RE3G. The aptamers specifically reduce the amount of His-Ix2CT complexed to GST-Ix3CT. The immunoblot was probed with an anti-penta-His antibody. 'Pool', pool 0 RNA; '-RNA', without RNA; 'GST', GST negative control.

ments using surface plasmon resonance (Lehmann et al., 2006). Thus, the interaction observed between GST-Ix3CT and Myc-Ix2 is likely due to an interaction with the innexin 2CL and/or the innexin 2CT. Both interactions might also occur in heteromeric hemichannels *in vivo*.

We next analyzed the interaction between innexin 2CT and innexin 3CT using purified proteins. His-Ix2CT associated with GST-Ix3CT, but only poorly with GST alone (Figure 7B). These results confirm the interaction of the CT of these innexins and provide a good experimental basis to investigate the effect of the selected aptamers on this interaction. We analyzed three different selected RNA molecules, RE3A, RE3G, and FS2. As a negative control we used the unselected pool. The presence of RE3A, RE3G or FS2 RNA in the pull-down mixture led to a clear decrease in the amount of complex formed between the CTs of innexin 3 and Myc-tagged innexin 2 (Figure 7C). In contrast, the unselected pool had no effect on the pull-down efficiency of the Ix3/Ix2 complex. The 2′-fluoro-modified FS2 RNA showed the most pronounced decrease in the amount of complex formed. The same result was obtained when Myc-tagged full-length innexin 2 was replaced by the histidine-tagged innexin 2 CT domain. Again, the unselected pool had no effect on the pull-down efficiency of the complexation of the two CT domains, whereas both RE3A and RE3G reduced the pull-down efficiency of the Ix3/Ix2 complex. GST alone was unable to bind to His-Ix2CT (Figure 7D). Thus, all re-selected aptamers and FS2 efficiently inhibit the interaction between the CTs of innexin 2 and innexin 3.

Discussion

Gap junction proteins possess a conserved topology and the sequences of the innexin family members within a species are highly homologous. Within the eight innexins present in *D. melanogaster*, innexin 2 is the smallest, with 367 amino acids and a molecular weight of 42.5 kDa (Bauer et al., 2005). By P-element insertion, *Drosophila* lines with defects in the *inx2* transcriptional unit were generated and isolated (Bauer et al., 2002). Two-thirds of these *kropf* mutants were embryonic lethal. Mutant embryos were growth-retarded and exhibited segment defects and holes in the epidermis of the head region. Few mutants developed to larval state, but exhibited a severe feeding defect due to a misshapen proventriculus. Immunohistochemical data showed that innexin 2 is distributed ubiquitously in epidermal epithelial cells in normal embryos (Bauer et al., 2003). The protein accumulates in apico-lateral membrane domains and in the cytoplasm. Yeast two-hybrid screens identified DE-cadherin, coracle, and armadillo as interaction partners for the intracellular domains of innexin 2 (Bauer et al., 2002, 2006; Lehmann et al., 2006). Innexin 2 co-localizes with armadillo and DE-cadherin in the embryonal epidermis. In *kropf* mutants, however, DE-cadherin and armadillo are mislocalized. Genetic evidence showed that a wingless signal activated innexin 2 transcription. During morphogenesis of the gut, wingless induces *inx2* expression at the ectoderm/endoderm transition, and this signal is required for proventriculus formation (Bauer et al., 2002).

While the *kropf* phenotype suggested a profound role of gap junction proteins in morphogenesis and other cellular processes, several aspects remain that are unclear and require further studies. For example, the molecular basis for functional differences among the various innexins still remains elusive, particularly in light of their high homology. The biological importance of heteromeric and homomeric channel formation is still unknown. Functional differences between individual members of the innexin family might be due to differences in the less conserved protein domains, i.e., the intracellular loop and the CT. Functional studies focusing on the activity of these domains would strongly benefit from the availability of inhibitors specifically targeting individual innexin domains. Therefore, the RNA aptamers described here that selectively target an innexin 2 cytoplasmic CT domain represent a first step towards this goal.

The anti-innexin 2 aptamers isolated in this study represent the first example of aptamers that target a cytoplasmic domain of a transmembrane protein that passes through the plasma membrane several times. So far, aptamers binding to cytoplasmic domains of transmembrane proteins have been described only for single transmembrane proteins, or for extracellular domains of single- or multi-transmembrane proteins. For example, whole-cell SELEX has yielded aptamers targeting extracellular domains (Pestourie et al., 2005) such as the RET receptor tyrosine kinase (Cerchia et al., 2005), tenascin C (Daniels et al., 2003), and the γ-aminobutyric acid (GABA) receptor (Cui et al., 2004). Examples of intracellular domains of single-transmembrane proteins include the $\alpha_L\beta_2$-integrin domain LFA1 (Blind et al., 1999) and β-

secretase BACE1 (Rentmeister et al., 2006), among others (Famulok and Verma, 2002). Furthermore, we report here one of the few examples in which an aptamer, the 2′-F-modified aptamer FS2, was initially selected for binding to a relatively short peptide epitope while still being able to recognize the full-length protein or an entire protein domain. Other examples that yielded protein-specific aptamers from selections with short peptide epitopes include the NS3 protease domain of hepatitis C virus (Urvil et al., 1997) and the prion protein (Proske et al., 2002a).

The other aptamers isolated in the initial selection only bound to the biotinylated peptide epitope 1 (Bio-Ix2CTept1), immobilized on streptavidin, providing an example of aptamers that require streptavidin as a 'hapten' for tight binding. These aptamers are not streptavidin binders; they require the immobilized Bio-Ix2CT-epitope, do not bind streptavidin alone and do not share any sequence homologies to known streptavidin-binding aptamers (Srisawat and Engelke, 2001). Consequently, it was possible to evolve members of the selected sequences into aptamers that recognize the innexin 2-CT domain alone, without requiring streptavidin. Filter-binding experiments confirmed that His-Ix2CT is bound by the evolved sequences RE3A and RE3G with apparent affinities of 308 and 222 nM, respectively. The re-selected sequences differ significantly from the sequences they were originally derived from, although the mutation rate of approximately 2% per base is moderate, and leads, on average, to 1–2 point mutations per 40-mer sequence. Sequence comparison of OU1 with the re-selected aptamers RE3A and RE3G shows that only 18 of the 39 positions in RE3A are identical to OU1, and 14 of the 40 positions in RE3G are identical to OU1. Interestingly, however, the consensus motifs observed in all selected sequences, including the 2′-fluoro-modified FS2, remained conserved in the re-selected sequences, suggesting that these motifs are important for binding. Furthermore, this finding also indicates that parts of the Ix2CTept1 peptide still belong to the binding epitope recognized by RE3A and RE3G. These sequences can recognize innexin 2 in the context of the full-length protein, as indicated by the pull-down experiments with the *in vitro*-translated Myc-innexin 2 and with His_6-Xa-tagged innexin 2CT. The His-tag and the protease factor Xa cleavage site are not utilized as 'haptens' for binding.

The affinity of these aptamers lies within a range that is often observed for aptamers that bind protein domains. Tight-binding aptamers have previously been observed that preferentially evolve to epitopes containing positively charged amino-acid residues, presumably utilizing electrostatic interactions (Nieuwlandt et al., 1995; Kimoto et al., 1998; Blind et al., 1999). Indeed, the epitope for which our selection was successful, Ix2CTept1, contains the highest number of positively charged amino-acid residues found in the complete CT domain of innexin 2, namely four arginines and one lysine residue.

Importantly, the selected aptamers interfere with the interaction of the CTs of innexins 2 and 3 (Figure 7C,D). This interaction was previously quantified *in vitro* by surface plasmon resonance measurements using the three immobilized innexin 3 cytoplasmic NT, loop, and CT domains, as well as the His_6-Xa-tagged innexin 2CT. It was also shown by biochemical fractionation experiments and co-immunostaining that innexin 2 and innexin 3 form heterodimers *in vivo* during the assembly of heteromeric channels. These data suggest that innexin heteromerization is crucial for epithelial tissue morphogenesis and polarity in *Drosophila* epidermis development. Furthermore, the binding of the two innexins via their CT domains provides a mechanism for oligomerization of heteromeric channels (Lehmann et al., 2006). The dissociation constant by which the CTs of the two innexins bind to each other *in vitro* was in the low micromolar range (K_d=2.45 μM). This affinity is in a range that appears suitable for interference with an inhibitory aptamer that binds to one of the interacting domains, namely Ix2CT, with approximately 10-fold better affinity (Table 2). The aptamers described here might be suitable inhibitors for targeting the innexin 2 CT domain in an *in vivo* environment in *Drosophila* embryos or larvae. In particular, the 2′-fluoro-modified FS2-47 sequence might be suitable for this purpose, not only because it is the sequence with the highest activity in interfering with heteromerization *in vitro* (Figure 7C), but also because of the generally increased stability of chemically modified aptamers (Kubik et al., 1997; Pagratis et al., 1997; Ruckman et al., 1998). We will report on the *in vivo* applications of these aptamers in due course.

Materials and methods

Materials

The peptides Bio-Ix2CTept1 and Bio-Ix2CTept2 were purchased from Jerini AG (Berlin, Germany), streptavidin was from Sigma-Aldrich GmbH (Munich, Germany), Ultralink streptavidin agarose was from Pierce Biotech, Inc. (Rockford, IL, USA), and the anti-penta-His-antibody was from Qiagen AG (Hilden, Germany).

Protein expression and purification

His- and GST-fusion proteins used in this study, as well as GST, were overexpressed in *Escherichia coli* from expression vectors described elsewhere (Lehmann et al., 2006). GST proteins from lysates were purified on glutathione-Sepharose according to the manufacturer's instructions (Amersham, Freiburg, Germany). Purified GST-fusion proteins were desalted, followed by dialysis against binding buffer (PBS, 3 mM $MgCl_2$, pH 7.4) to remove free and bound glutathione. The proteins containing an N-terminal His6-tag were purified by standard Ni^{2+}-NTA affinity chromatography and dialyzed against binding buffer.

RNA library design and construction

The synthetic ssDNA library 5′-TCT AAT ACG ACT CAC TAT AGG GAG AGA CAA GCT TGG GTC-N40-CTC TTG CTC TTC CTA GGA GT-3′ (where N40 is the randomized part) was amplified using the selection primers P20I (5′-ACT CCT AGG AAG AGC AAG AG-3′) and P39F (5′-TCT AAT ACG ACT CAC TAT AGG GAG AGA CAA GCT TGG GTC-3′). A double-stranded DNA pool was generated from the original synthetic oligomer by large-scale PCR, and an RNA pool was transcribed from a portion (approx. 10^{14} sequences) of this pool. *In vitro* transcription with T7 RNA polymerase yielded the corresponding RNA library. In selections with the 2′-fluoro-2′-deoxy-modified RNAs, *in vitro* transcription was performed in the presence of 2′-fluoro-2′-

deoxy-pyrimidine triphosphates using the T7 RNA polymerase mutant Y639P (Sousa and Padilla, 1995).

In vitro selection of aptamers

Selections were carried out as previously described (Blind et al., 1999). In particular, internally [^{32}P]-labeled RNA (10 nmol in cycle 1, 2 nmol in subsequent cycles) was incubated with biotin-Ix2CTept1/streptavidin agarose in selection buffer (4.3 mM Na_2HPO_4, 1.4 mM KH_2PO_4, 2.7 mM KCl, 147 mM NaCl, 3.0 mM $MgCl_2$, pH7.4) with 0.8 U/μl RNasin for 30 min at 25°C. After washing with selection buffer, binding species were eluted with denaturing buffer (30 mM Tris, 5 mM EDTA, 6 M guanidine hydrochloride, pH 7.4). Eluted RNA was amplified as previously described (Klug et al., 1997).

Error-prone PCR (EP-PCR)

EP-PCR was carried out according to Cadwell and Joyce (1994). To mutagenize the aptamers OU1 and OU3, 200 ng of DNA was amplified for 15 cycles in a 100-μl EP-PCR mixture (10 mM Tris, pH 8.3, 50 mM KCl, 7 mM $MgCl_2$, 1 mM dCTP, 1 mM dTTP, 0.2 mM dATP, 0.2 mM dGTP, 2 μM 5′-pimer, 2 μM 3′-primer, 0.5 mM $MnCl_2$, 0.05 U/μl Taq DNA polymerase from Promega (Mannheim, Germany). Before final extension at 72°C was completed, 1 μl of the EP-PCR reaction was transferred to a new preheated tube containing 99 μl of EP-PCR mixture and again amplified for 15 PCR cycles. Thermocycling was at 94°C for 60 s, 55°C for 60 s, and 72°C for 60 s. For the re-selection library, DNAs of OU1 and OU3 mutagenesis were mixed 1:1.

Re-selection

For re-selection, internally [^{32}P]-labeled RNA (2 nmol) was incubated with GST-Ix2CT and selected with 1.6 U/μl RNasin for 30 min at 25°C. The GST fusion protein was captured on glutathione-Sepharose (Amersham). After washing with selection buffer, bound RNAs were eluted by competition with 5 μM His-Ix2CT in binding buffer and amplified as described earlier.

Filter binding assays

Filter binding was performed as described by Proske et al. (2002b). Essentially, binding studies were performed with 1 nM 5′-[^{32}P]-labeled RNA. In Bio-Ix2CTept binding assays, RNA was incubated with a peptide dilution series ranging from 1 nM to 10 μM in 50 μl of binding buffer plus 20 μg/ml streptavidin to improve retention on the nitrocellulose filter and 1% heparin for 30 min at 25°C. His-Ix2CT binding studies were performed with 25 nM to 2–5 μM His-Ix2CT and 1 μM *E. coli* tRNA. The percentage RNA retained on each filter was quantified by PhosphorImaging.

Pull-down and inhibition assays

A coupled TNT transcription/translation kit (Promega) was used according to the manufacturer's instructions and supplemented with [^{35}S]-Pro-mix to produce *in vitro* translated proteins from constructs described elsewhere (Lehmann et al., 2006). In the aptamer binding assays, 5′-biotinylated RNAs were incubated with 2 μl of translation mix in 25 μl of binding buffer for 30 min at 25°C. RNAs were captured on streptavidin agarose. For GST pull-down assays, equimolar amounts of GST and GST-fusion proteins using 400–540 ng of protein were immobilized on 10 μl of glutathione-Sepharose by incubation for 4 h at 25°C in binding buffer plus 1 mM DTT, 1 μg/μl BSA and 2 μg/μl salmon sperm DNA. Beads were washed with binding buffer prior to addition of either 10 μl of translation mix or His-Ix2CT at a final concentration of 600 nM. In the inhibition assays, 1 μM RNAs (Myc-Ix2) or 2 μM RNAs (His-Ix2CT) was incubated with proteins in binding buffer with 0.8 U/μl RNasin for 15 min prior to the addition of GST-Ix3CT captured on GST-Sepharose. Incubation was carried out for 1 h at 25°C. The total volume of binding mixtures in GST pull-down assays was 100 μl. All matrixes were washed with binding buffer and bound proteins were eluted with Laemmli buffer. Eluates were separated by SDS-PAGE and proteins were detected using autoradiography or after Western blotting with anti-penta-His antibody.

Acknowledgments

This work was supported by Graduiertenkolleg 804 and Sonderforschungsbereich SFB 645. We thank Ulrich Wüllner and Michael Weyler for their contributions to this project.

References

Ai, Z., Fischer, A., Spray, D.C., Brown, A.M., and Fishman, G.I. (2000). Wnt-1 regulation of connexin43 in cardiac myocytes. J. Clin. Invest. *105*, 161–171.

Anumonwo, J.M., Taffet, S.M., Gu, H., Chanson, M., Moreno, A.P., and Delmar, M. (2001). The carboxyl-terminal domain regulates the unitary conductance and voltage dependence of connexin40 gap junction channels. Circ. Res. *88*, 666–673.

Bauer, R., Lehmann, C., Fuss, B., Eckardt, F., and Hoch, M. (2002). The *Drosophila* gap junction channel gene innexin 2 controls foregut development in response to Wingless signalling. J. Cell Sci. *115*, 1859–1867.

Bauer, R., Martini, J., Lehmann, C., and Hoch, M. (2003). Cellular distribution of innexin 1 and 2 gap junctional channel proteins in epithelia of the *Drosophila* embryo. Cell Commun. Adhes. *10*, 221–225.

Bauer, R., Lehmann, C., Martini, J., Eckardt, F., and Hoch, M. (2004). Gap junction channel protein innexin 2 is essential for epithelial morphogenesis in the *Drosophila* embryo. Mol. Biol. Cell *15*, 2992–3004.

Bauer, R., Loer, B., Ostrowski, K., Martini, J., Weimbs, A., Lechner, H., and Hoch, M. (2005). Intercellular communication: the *Drosophila* innexin multiprotein family of gap junction proteins. Chem. Biol. *12*, 515–526.

Bauer, R., Weimbs, A., Lechner, H., and Hoch, M. (2006). DE-cadherin, a core component of the adherens junction complex modifies subcellular localization of the *Drosophila* gap junction protein innexin2. Cell Commun. Adhes. *13*, 103–114.

Blind, M., Kolanus, W., and Famulok, M. (1999). Cytoplasmic RNA modulators of an inside-out signal-transduction cascade. Proc. Natl. Acad. Sci. USA *96*, 3606–3610.

Bruzzone, R., Hormuzdi, S.G., Barbe, M.T., Herb, A., and Monyer, H. (2003). Pannexins, a family of gap junction proteins expressed in brain. Proc. Natl. Acad. Sci. USA *100*, 13644–13649.

Cadwell, R.C. and Joyce, G.F. (1992). Randomization of genes by PCR mutagenesis. PCR Methods Appl. *2*, 28–33.

Cadwell, R.C. and Joyce, G.F. (1994). Mutagenic PCR. PCR Methods Appl. *3*, S136–140.

Cerchia, L., Duconge, F., Pestourie, C., Boulay, J., Aissouni, Y., Gombert, K., Tavitian, B., de Franciscis, V., and Libri, D. (2005). Neutralizing aptamers from whole-cell SELEX inhibit the RET receptor tyrosine kinase. PLoS Biol. *3*, e123.

Choi, K.H., Park, M.W., Lee, S.Y., Jeon, M.Y., Kim, M.Y., Lee, H.K., Yu, J., Kim, H.J., Han, K., Lee, H., et al. (2006). Intracellular expression of the T-cell factor-1 RNA aptamer as an intramer. Mol. Cancer Ther. *5*, 2428–2434.

Cui, Y., Rajasethupathy, P., and Hess, G.P. (2004). Selection of stable RNA molecules that can regulate the channel-opening equilibrium of the membrane-bound γ-aminobutyric acid receptor. Biochemistry *43*, 16442–16449.

Daniels, D.A., Chen, H., Hicke, B.J., Swiderek, K.M., and Gold, L. (2003). A tenascin-C aptamer identified by tumor cell SELEX: systematic evolution of ligands by exponential enrichment. Proc. Natl. Acad. Sci. USA *100*, 15416–15421.

Duffy, H.S., Delmar, M., Coombs, W., Tafftet, S.M., Hertzberg, E.L., and Spray, D.C. (2001). Functional demonstration of connexin-protein binding using surface plasmon resonance. Cell Commun. Adhes. *8*, 225–229.

Duffy, H.S., Sorgen, P.L., Girvin, M.E., O'Donnell, P., Coombs, W., Taffet, S.M., Delmar, M., and Spray, D.C. (2002). pH-dependent intramolecular binding and structure involving Cx43 cytoplasmic domains. J. Biol. Chem. *277*, 36706–36714.

Famulok, M. and Mayer, G. (2005). Intramers and aptamers: applications in protein-function analyses and potential for drug screening. ChemBioChem *6*, 19–26.

Famulok, M. and Verma, S. (2002). *In vivo*-applied functional RNAs as tools in proteomics and genomics research. Trends Biotechnol. *20*, 462–466.

Giepmans, B.N. and Moolenaar, W.H. (1998). The gap junction protein connexin43 interacts with the second PDZ domain of the zona occludens-1 protein. Curr. Biol. *8*, 931–934.

Giepmans, B.N., Verlaan, I., and Moolenaar, W.H. (2001). Connexin-43 interactions with ZO-1 and α- and β-tubulin. Cell Commun. Adhes. *8*, 219–223.

Kimoto, M., Sakamoto, K., Shirouzu, M., Hirao, I., and Yokoyama, S. (1998). RNA aptamers that specifically bind to the Ras-binding domain of Raf-1. FEBS Lett. *441*, 322–326.

Klug, S.J., Hüttenhofer, A., Kromayer, M., and Famulok, M. (1997). *In vitro* and *in vivo* characterization of novel mRNA motifs that bind special elongation factor SelB. Proc. Natl. Acad. Sci. USA *94*, 6676–6681.

Kubik, M.F., Bell, C., Fitzwater, T., Watson, S.R., and Tasset, D.M. (1997). Isolation and characterization of 2′-fluoro-, 2′-amino-, and 2′-fluoro-/amino-modified RNA ligands to human IFN-γ that inhibit receptor binding. J. Immunol. *159*, 259–267.

Kumar, N.M. and Gilula, N.B. (1996). The gap junction communication channel. Cell *84*, 381–388.

Lehmann, C., Lechner, H., Loer, B., Knieps, M., Herrmann, S., Famulok, M., Bauer, R., and Hoch, M. (2006). Heteromerization of innexin gap junction proteins regulates epithelial tissue organization in *Drosophila*. Mol. Biol. Cell *17*, 1676–1685.

Lin, Y., Qiu, Q., Gill, S.C., and Jayasena, S.D. (1994). Modified RNA sequence pools for *in vitro* selection. Nucleic Acids Res. *22*, 5229–5234.

Martin, P.E. and Evans, W.H. (2004). Incorporation of connexins into plasma membranes and gap junctions. Cardiovasc. Res. *62*, 378–387.

Mayer, G., Blind, M., Nagel, W., Bohm, T., Knorr, T., Jackson, C.L., Kolanus, W., and Famulok, M. (2001). Controlling small guanine-nucleotide-exchange factor function through cytoplasmic RNA intramers. Proc. Natl. Acad. Sci. USA *98*, 4961–4965.

Nieuwlandt, D., Wecker, M., and Gold, L. (1995). *In vitro* selection of RNA ligands to substance P. Biochemistry *34*, 5651–5659.

Pagratis, N.C., Bell, C., Chang, Y.-F., Jennings, S., Fitzwater, T., Jellinek, D., and Dang, C. (1997). Potent 2′-amino-, and 2′-fluoro-2′-deoxyribonucleotide RNA inhibitors of keratinocyte growth factor. Nat. Biotechnol. *15*, 68–73.

Pestourie, C., Tavitian, B., and Duconge, F. (2005). Aptamers against extracellular targets for *in vivo* applications. Biochimie *87*, 921–930.

Phelan, P., Bacon, J.P., Davies, J.A., Stebbings, L.A., Todman, M.G., Avery, L., Baines, R.A., Barnes, T.M., Ford, C., Hekimi, S., et al. (1998). Innexins: a family of invertebrate gap-junction proteins. Trends Genet. *14*, 348–349.

Phelan, P. and Starich, T.A. (2001). Innexins get into the gap. Bioessays, *23*, 388–396.

Pieken, W.A., Olsen, D.B., Benseler, F., Aurup, H., and Eckstein, F. (1991). Kinetic characterization of ribonuclease-resistant 2′-modified hammerhead ribozymes. Science *253*, 314–317.

Proske, D., Gilch, S., Wopfner, F., Schatzl, H.M., Winnacker, E.L., and Famulok, M. (2002a). Prion-protein-specific aptamer reduces PrPSc formation. ChemBioChem *3*, 717–725.

Proske, D., Hofliger, M., Soll, R.M., Beck-Sickinger, A.G., and Famulok, M. (2002b). A Y2 receptor mimetic aptamer directed against neuropeptide Y. J. Biol. Chem. *277*, 11416–11422.

Reader, J.S. and Joyce, G.F. (2002). A ribozyme composed of only two different nucleotides. Nature *420*, 841–844.

Rentmeister, A., Bill, A., Wahle, T., Walter, J., and Famulok, M. (2006). RNA aptamers selectively modulate protein recruitment to the cytoplasmic domain of β-secretase BACE1 *in vitro*. RNA *12*, 1650–1660.

Rogers, J. and Joyce, G.F. (1999). A ribozyme that lacks cytidine. Nature *402*, 323–325.

Rogers, J. and Joyce, G.F. (2001). The effect of cytidine on the structure and function of an RNA ligase ribozyme. RNA *7*, 395–404.

Ruckman, J., Green, L.S., Beeson, J., Waugh, S., Gillette, W.L., Henninger, D.D., Claesson, W.L., and Janjic, N. (1998). 2′-Fluoropyrimidine RNA-based aptamers to the 165-amino acid form of vascular endothelial growth factor (VEGF165). Inhibition of receptor binding and VEGF-induced vascular permeability through interactions requiring the exon 7-encoded domain. J. Biol. Chem. *273*, 20556–20567.

Schubert, A.L., Schubert, W., Spray, D.C., and Lisanti, M.P. (2002). Connexin family members target to lipid raft domains and interact with caveolin-1. Biochemistry *41*, 5754–5764.

Segretain, D. and Falk, M.M. (2004). Regulation of connexin biosynthesis, assembly, gap junction formation, and removal. Biochim. Biophys. Acta *1662*, 3–21.

Shi, H., Hoffman, B.E., and Lis, J.T. (1999). RNA aptamers as effective protein antagonists in a multicellular organism. Proc. Natl. Acad. Sci. USA *96*, 10033–10038.

Söhl, G. and Willecke, K. (2004). Gap junctions and the connexin protein family. Cardiovasc. Res. *62*, 228–232.

Sorgen, P.L., Duffy, H.S., Sahoo, P., Coombs, W., Delmar, M., and Spray, D.C. (2004). Structural changes in the carboxyl terminus of the gap junction protein connexin43 indicates signaling between binding domains for c-Src and zonula occludens-1. J. Biol. Chem. *279*, 54695–54701.

Sousa, R. and Padilla, R. (1995). A mutant T7 RNA polymerase as a DNA polymerase. EMBO J. *14*, 4609–4621.

Srisawat, C. and Engelke, D.R. (2001). Streptavidin aptamers: affinity tags for the study of RNAs and ribonucleoproteins. RNA *7*, 632–641.

Stebbings, L.A., Todman, M.G., Phillips, R., Greer, C.E., Tam, J., Phelan, P., Jacobs, K., Bacon, J.P., and Davies, J.A. (2002). Gap junctions in *Drosophila*: developmental expression of the entire innexin gene family. Mech. Dev. *113*, 197–205.

Theis, M.G., Knorre, A., Kellersch, B., Moelleken, J., Wieland, F., Kolanus, W., and Famulok, M. (2004). Discriminatory aptamer reveals serum response element transcription regulated by cytohesin-2. Proc. Natl. Acad. Sci. USA *101*, 11221–11226.

Toyofuku, T., Akamatsu, Y., Zhang, H., Kuzuya, T., Tada, M., and Hori, M. (2001). c-Src regulates the interaction between connexin-43 and ZO-1 in cardiac myocytes. J. Biol. Chem. *276*, 1780–1788.

Urvil, P.T., Kakiuchi, N., Zhou, D.M., Shimotohno, K., Kumar, P.K., and Nishikawa, S. (1997). Selection of RNA aptamers that bind specifically to the NS3 protease of hepatitis C virus. Eur. J. Biochem. *248*, 130–138.

Zuker, M. (2003). Mfold web server for nucleic acid folding and hybridization prediction. Nucleic Acids Res. *31*, 3406–3415.

Received February 27, 2007; accepted March 19, 2007